Published in final edited form as:
Nature. 2010 July 29; 466(7306): 622–626. doi:10.1038/nature09159.

Regulation of parkinsonian motor behaviors by optogenetic control of basal ganglia circuitry

Alexxai V. Kravitz[1], **Benjamin S. Freeze**[1,4,5], **Philip R.L. Parker**[1,3], **Kenneth Kay**[1,5], **Myo T. Thwin**[1], **Karl Deisseroth**[6], and **Anatol C. Kreitzer**[1,2,3,4,5,*]

[1]Gladstone Institute of Neurological Disease, University of California, San Francisco

[2]Departments of Physiology and Neurology, University of California, San Francisco

[3]Neuroscience Graduate Program, University of California, San Francisco

[4]Biomedical Sciences Program, University of California, San Francisco

[5]Medical Scientist Training Program, University of California, San Francisco

[6]Departments of Bioengineering and Psychiatry and Behavioral Sciences, Stanford University

Abstract

Neural circuits of the basal ganglia are critical for motor planning and action selection[1-3]. Two parallel basal ganglia pathways have been described[4], which are proposed to exert opposing influences on motor function[5-7]. According to this classical model, activation of the direct pathway facilitates movement and activation of the indirect pathway inhibits movement. However, more recent anatomical and functional evidence has called into question the validity of this hypothesis[8-10]. Because this model has never been empirically tested, the specific function of these circuits in behaving animals remains unknown. Here, we directly activated basal ganglia circuitry *in vivo*, using optogenetic control[11-14] of direct- and indirect-pathway medium spiny projection neurons (MSNs), achieved through Cre-dependent viral expression of channelrhodopsin-2 in the striatum of D1-Cre and D2-Cre BAC transgenic mice. Bilateral excitation of indirect-pathway MSNs elicited a parkinsonian state, distinguished by increased freezing, bradykinesia, and decreased locomotor initiations. In contrast, activation of direct-pathway MSNs reduced freezing and increased locomotion. In a mouse model of Parkinson's disease, direct pathway activation completely rescued deficits in freezing, bradykinesia, and locomotor initiation. Taken together, our findings establish a critical role for basal ganglia circuitry in the bidirectional regulation of motor behavior and indicate that modulation of direct pathway circuitry may represent an effective therapeutic strategy for ameliorating parkinsonian motor deficits.

To obtain selective optogenetic control of the direct and indirect pathways *in vivo*, we targeted striatal MSNs that form the origin of these pathways. We injected an adeno-associated virus (AAV1) containing a double-floxed inverted open reading frame (DIO)

* To whom correspondence should be addressed: Gladstone Institute of Neurological Disease 1650 Owens St. San Francisco, CA 94158 Tel: 415-734-2507 Fax: 415-355-0824 akreitzer@gladstone.ucsf.edu.

Author Contributions A.V.K., P.R.L.P., and M.T.T. collected and processed tissue, and analyzed immunohistochemical experiments. B.S.F. performed and analyzed in vitro electrophysiology experiments. A.V.K., B.S.F., and P.R.L.P. performed and analyzed in vivo electrophysiology experiments. A.V.K., P.R.L.P., and K.K. performed and analyzed optogenetic/behavioral experiments. K.D. provided Cre-dependent ChR2-YFP and YFP-control constructs. A.C.K. designed and coordinated the study, and A.C.K. and A.V.K wrote the paper.

The authors declare no competing financial interests.

Supplementary Information is linked to the online version of the paper at www.nature.com/nature

encoding a fusion of channelrhodopsin-2 and enhanced yellow fluorescent protein (ChR2-YFP)[15, 16] (Fig. 1a) into the dorsomedial striatum of BAC transgenic mice expressing Cre-recombinase (Cre) in direct- or indirect-pathway MSNs (D1-Cre and D2-Cre, respectively)[17]. Functional ChR2-YFP is transcribed only in neurons containing Cre, thus restricting expression to either direct- or indirect-pathway MSNs. Dorsomedial striatum was chosen as a target because it is thought to be involved in earlier stages of motor processing[1] and thus would be more likely to yield global changes in motor behavior. To confirm the expression pattern of ChR2 in the dorsomedial striatum, we prepared sagittal sections at two weeks post-injection that included the striatum, globus pallidus (GP), and substantia nigra pars reticulata (SNr) (Fig. 1b). In D1-Cre mice, numerous ChR2-YFP-positive cell bodies were observed in the striatum, along with fibers traversing the GP that projected to the entopeduncular nucleus (EP) and SNr (Fig. 1c), the canonical targets of direct-pathway MSNs. In D2-Cre mice, ChR2-YFP-positive cell bodies were observed in the striatum, and fibers projected to the GP, but not the EP or SNr, consistent with proper targeting of ChR2-YFP to indirect-pathway MSNs (Fig. 1d). Immunostaining for Cre and the MSN marker DARPP-32[18] confirmed that the vast majority (>90%) of ChR2-YFP-positive cells expressed both Cre and DARPP-32 (Supp. Fig. 1, Supp. Table 1). To investigate whether ChR2-YFP was expressed in striatal interneurons, we immunostained each line for choline acetyltransferase (ChAT), parvalbumin (PV), and neuropeptide Y (NPY) (Fig. 1e-g), markers of cholinergic, fast-spiking, and low-threshold spiking interneurons, respectively[19]. Very few (<5%) interneurons expressed ChR2-YFP (Fig. 1g; Supp. Table 1). These findings were confirmed electrophysiologically, by comparing the passive and active membrane properties of ChR2-YFP-positive neurons with the properties of known striatal neuron subtypes[20]. All recorded neurons exhibited characteristics of MSNs (Supp. Fig. 2, Supp. Table 1). We found no evidence for expression of ChR2-YFP in striatal afferent fibers from either the substantia nigra pars compacta (Supp. Fig. 3) or cortex (Supp. Fig. 4).

In order to confirm that ChR2-YFP expression alone did not alter the electrophysiological properties of MSNs, we performed whole-cell recordings in brain slices prepared from D1- or D2-Cre mice injected with ChR2-YFP virus (subsequently referred to as D1-ChR2 and D2-ChR2 mice, respectively). The current-firing relationships for direct- and indirect-pathway MSNs expressing ChR2-YFP were not significantly different from control MSNs (D1-ChR2 vs. control, $p>0.30$ for all points; D2-ChR2 vs. control, $p>0.26$ for all points; Fig. 2a, b), and ChR2-YFP expression did not significantly change the passive properties of MSNs (Supp. Table 2). However, consistent with previous reports[21], D1-ChR2-positive MSNs were significantly less excitable than D2-ChR2-positive MSNs, providing further evidence that these subpopulations were selectively labeled by ChR2-YFP. 470 nm illumination of ChR2-YFP-positive MSNs elicited large light-evoked currents in voltage-clamp, and robust spiking in current-clamp (Fig. 2c, d), indicating that ChR2 was functional in these neurons.

We next tested ChR2 function *in vivo* in the striatum of anesthetized D1- and D2-ChR2 mice. Recordings were performed with an optrode[22] that consisted of a linear 16-site silicon probe with an integrated laser-coupled optical fiber that could elicit light-induced spiking at least 800 μm from the fiber tip (Supp. Fig. 5). In both mouse lines, we observed significant firing rate increases in approximately 35% of recorded neurons during 473 nm laser illumination (1 mW at fiber tip) (Fig. 2e-h), although this is likely an overestimate of the actual percentage of ChR2-positive MSNs. We considered the possibility that illumination recruited previously silent neurons that could infiltrate the recording and bias our quantification of firing rate changes. However, we observed no difference in the spike waveforms during illumination (see Fig. 2f, g insets), nor did light-induced spikes occur within the refractory period of the recorded neuron, indicating that no additional units were recruited. Overall, average MSN firing rates in D1-ChR2 mice increased from 0.03Hz to

1.16Hz with illumination; in D2-ChR2 mice, average firing rates increased from 0.06Hz to 0.76Hz with illumination (D1-ChR2, n=16, $p<0.0001$; D2-ChR2, n=10, $p<0.005$). The light-induced firing rate of MSNs (~1Hz) was well below the maximal firing rate of MSNs, indicating that we did not drive these neurons strongly under anesthetized conditions. However, basal MSN firing rates under anesthesia were approximately 10-fold lower then those observed in awake mice, suggesting that our light-induced firing rate changes may not reflect the efficacy of optical stimulation in awake mice.

According to the classical model of basal ganglia function, selective expression of dopamine D1 and D2 receptors in the direct and indirect pathways, respectively, enables differential modulation of direct- and indirect-pathway MSNs[5, 23]. To experimentally test this hypothesis, we recorded from optically-identified direct- or indirect-pathway MSNs *in vivo* and administered D1 or D2 agonists. However, no consistent effects were observed (Supp. Fig. 6), highlighting the complexity of pharmacological modulation in intact circuits.

To confirm that activation of direct- or indirect-pathway MSNs can drive activity in basal ganglia circuits *in vivo*, we next performed recordings in the main basal ganglia output nucleus (SNr) during striatal illumination in D1- or D2-ChR2 mice (Fig. 2i). In SNr regions innervated by optically-stimulated MSNs (as assessed by local field potential modulation), 8/10 of SNr neurons responded to direct pathway activation, whereas 4/11 of SNr neurons responded to indirect pathway activation (Supp. Fig. 7). All responsive SNr neurons displayed robust changes in firing rate (D1-ChR2 mice: 8.6±3.0% of baseline firing rate, n=8; D2-ChR2 mice: 162±19% of baseline firing rate, n=4) that were consistent with the classical model: direct pathway activation inhibited firing of SNr neurons, whereas indirect pathway activation excited SNr neurons (Fig. 2j-l).

After verifying the expression pattern of ChR2 in the direct or indirect pathways, and confirming our ability to drive direct and indirect pathway basal ganglia circuits *in vivo*, we examined the behavioral effects of activating basal ganglia circuits in awake mice. Cannulas were surgically implanted over dorsomedial striatum (Fig. 3a) and used to guide both viral injections and fiber optic placements. Unilateral illumination of dorsomedial striatum in D1- and D2-ChR2 mice elicited rotational behavior (Supp. Fig. 8; also see Supp. Movie 1). Direct pathway activation led to contraversive rotations, whereas indirect pathway activation yielded ipsiversive rotations. Thus, unilateral indirect pathway activation mimics rotational behavior induced by unilateral dopamine depletion[24], consistent with the classical model of basal ganglia function.

Bilateral illumination of direct-pathway MSNs elicited decreases in freezing and fine movements, and an increase in the percentage of time spent in ambulation (Figure 3b, c, n=9, $p<0.05$). In contrast, when we stimulated the indirect pathway, we observed decreases in ambulation and fine movements (n=8, $p<0.05$), and a sharp increase in the amount of time spent freezing (Fig. 3b, c, n=8, $p<0.001$; also see Supp. Movie 2). Changes in percentage of time spent performing fine movements were not correlated with changes in grooming frequency for either ChR2-expressing line (D1-ChR2, n=9, p=0.30, D2-ChR2, n=8, p=0.93). However, fine movements were more vigorous during direct pathway activation (increased centerpoint velocity) and less vigorous during indirect pathway activation (Fig. 3d; D1-ChR2, n=9, $p>0.005$, D2-ChR2, n=8, $p>0.05$). As a control, we injected Cre-dependent virus expressing only YFP (D1-YFP and D2-YFP mice). In these mice, we observed no difference in time spent ambulatory, freezing, or performing fine movements in either mouse line during illumination (n=5 for each line, $p>0.23$ for all conditions).

Next, we analyzed ambulation patterns during bilateral activation of the direct or indirect pathways (Fig. 3e-g). During illumination, D1-ChR2 mice initiated more frequent

ambulatory bouts (n=9, p<0.005), and these bouts lasted longer (n=9, p<0.05); no changes in ambulation velocity occurred (n=9, p=0.21). In contrast, indirect pathway activation led to less frequent initiation of ambulation (n=8, p<0.0005). When ambulation did occur, it lasted a shorter time (n=8, p<0.05) and had a lower velocity (n=8, p<0.0005). There were no differences on any measures of ambulation for the YFP-expressing controls during illumination (Supp. Fig. 9; n=5 for each line, p>0.35 for all measures). We then examined the frequency and duration of freezing bouts during illumination (Fig. 3h, i). D1-ChR2-expressing mice exhibited less frequent freezing bouts (n=9, p<0.05), and these bouts were shorter (n=9, p<0.0001). D2-ChR2 expressing mice had more frequent freezing bouts during illumination (n=8, p<0.05), and freezing bouts that did occur lasted much longer (n=8, p<0.05). There were no differences on either measure of freezing for the YFP-expressing controls during illumination (Supp. Fig. 9; n=5 for each line, p>0.20 for each measure). Together these data establish a causal role for the direct pathway in decreasing freezing and increasing locomotor initiations, and for the indirect pathway in increasing freezing, decreasing locomotor initations, and inducing bradykinesia.

In order to test whether changes in ambulation patterns reflected altered locomotor coordination, we examined gait parameters in D1- and D2-ChR2 mice in response to illumination, using a treadmill equipped with a high-speed camera. We quantified multiple gait parameters with the laser on and off, and found no significant differences in the average or variance of stride length, stance width, stride frequency, stance duration, swing duration, paw angle, and paw area on belt for either line (n=4 for D1-ChR2, n=5 for D2-ChR2, all p>0.05, Fig. 3j; Supp. Fig. 10). This indicates that activation of direct and indirect pathways in the dorsomedial striatum regulates the pattern of motor activity, without changing the coordination of ambulation itself.

Parkinsonian motor deficits are hypothesized to result from an overactive indirect pathway and an underactive direct pathway[5, 25-27]. Surgical treatments for PD are focused on reducing activity in the indirect pathway, through lesions or deep-brain stimulation. However, there has been no experimental test of whether increasing direct pathway activity in PD models can ameliorate parkinsonian motor symptoms. We tested this hypothesis using bilateral illumination of ChR2 in bilateral 6-OHDA-lesioned mice. 6-OHDA was injected bilaterally into the dorsomedial striatum, resulting in a near-total loss of dopaminergic innervation of this region after 1 week (Fig. 4a-b; TH intensity in dorsomedial striatum: 4±12% of control, n=4, p<0.005), which was accompanied by parkinsonian motor deficits that included bradykinesia (decreased fine movement velocity), decreased time spent ambulatory, decreased locomotor initiation, and increased freezing (both frequency and duration) (Fig. 4e-k; n=10, p<0.05 for all analyses). We attempted to rescue these symptoms using bilateral direct pathway activation in the same region of dorsomedial striatum that lacked dopamine innervation (Fig. 4c-d; also see Supp. Methods). Surprisingly, direct pathway activation completely restored motor behavior to pre-lesion levels (Fig. 4e-k). Direct pathway activation eliminated bradykinesia (increased fine movement velocity to pre-lesion levels, p<0.01), increased locomotor initiations (p<0.05), and decreased freezing (p<0.05). Changes in gait parameters were not observed after 6-OHDA or direct pathway activation (Figure 4l, p>0.14). Taken together, these findings provide the first evidence that direct pathway activation can ameliorate a constellation of motor deficits in a mouse model of PD. However, future studies utilizing a comprehensive battery of sensorimotor tests will be required to fully characterize the role of direct and indirect pathway circuit activity in motor function and dysfunction in PD.

In summary, our findings establish a causal role for direct- and indirect-pathway basal ganglia circuits in regulating motor behavior. Consistent with a role in action selection, activation of direct or indirect pathway circuitry altered the type of motor behaviors

performed, without disrupting motor coordination itself. Thus, one function of basal ganglia circuitry may be to translate changes in motivational state into appropriate levels of motor activity. In PD, loss of dopamine neurons impairs signaling of motivational state, even though the capacity for movement is maintained. Our studies suggest that activation of the direct pathway may represent a novel strategy for bypassing dopamine signaling and directly enhancing motor function in PD.

Methods Summary

Viral expression of DIO-ChR2-YFP in BAC transgenic mice

Injections of recombinant AAV1 virus targeted the dorsomedial striatum in BAC transgenic D1-Cre and D2-Cre (BAC) transgenic mice[17]. Double-floxed inverted (DIO) constructs encoding ChR2-YFP restricted expression to Cre-positive cells[15, 16].

Electrophysiology

For in vivo recordings, we coupled an 80 mW TTL-controlled 473nm laser to a silicon optrode (NeuroNexus) via a fiber optic patch cord, and attenuated laser power to yield 1 mW at the fiber tip. Recordings were performed using a 64-channel Multichannel Acquisition Processor (Plexon). Single units were discriminated with principal component analysis.

Optical stimulation and behavioral analysis in awake mice

Two 3-meter glass fibers (AFS105/125Y, Thorlabs) were connectorized with SMA connectors on one end, and cleaved flat on the other end, which were inserted through guide cannulas into the dorsomedial striatum. Laser power was adjusted to yield 1 mW at tip of each fiber. The position of the nose, tail, and center of mass of each mouse were tracked using Noldus Ethovision 6.0 software. Animals were recorded for a 1-10 minute baseline period before any laser illumination to obtain baseline behavioral measures. Following this period, the striatum was illuminated in a series of 10 trials. Each trial had a variable period during which the laser was on (constant illumination, 30 seconds average, 20-40 sec range), followed by a variable period where the laser was off (60 seconds average, 50-70 sec range).

6-OHDA treatment

Mice were cannulated and injected with ChR2-YFP as described above. Nine days following viral injection, ‘pre-lesion’ behavioral data was collected from these animals. Directly following this data collection, mice were anesthetized with ketamine and xylazine, and 6-OHDA (5mg/ml) was injected through the same cannulas as the virus (1μL/hemisphere). Mice were allowed to recover for 5 days before post-lesion behavioral testing.

Supplementary Material

Refer to Web version on PubMed Central for supplementary material.

Acknowledgments

We thank Timothy Marzullo and NeuroNexus Technologies for their assistance with the custom probe design, the Nikon Imaging Center at UCSF for assistance with image acquisition, Robyn Javier and Aryn Gittis for assistance with slice electrophysiology experiments, and Liza Shoenfeld for assistance with genotyping and histology. A.C.K and co-workers are funded by the W.M. Keck Foundation, the Pew Charitable Trusts, the McKnight Foundation, and the NIH.

References

1. Yin HH, Knowlton BJ. The role of the basal ganglia in habit formation. Nat. Rev. 2006; 7:464–476.
2. Hikosaka O, Takikawa Y, Kawagoe R. Role of the basal ganglia in the control of purposive saccadic eye movements. Physiol. Rev. 2000; 80:953–978. [PubMed: 10893428]
3. Graybiel AM, Aosaki T, Flaherty AW, Kimura M. The basal ganglia and adaptive motor control. Science. 1994; 265:1826–1831. [PubMed: 8091209]
4. Smith Y, Bevan MD, Shink E, Bolam JP. Microcircuitry of the direct and indirect pathways of the basal ganglia. Neuroscience. 1998; 86:353–387. [PubMed: 9881853]
5. Albin RL, Young AB, Penney JB. The functional anatomy of basal ganglia disorders. Trends Neurosci. 1989; 12:366–375. [PubMed: 2479133]
6. DeLong MR. Primate models of movement disorders of basal ganglia origin. Trends Neurosci. 1990; 13:281–285. [PubMed: 1695404]
7. Alexander GE, Crutcher MD. Functional architecture of basal ganglia circuits: neural substrates of parallel processing. Trends Neurosci. 1990; 13:266–271. [PubMed: 1695401]
8. Kawaguchi Y, Wilson CJ, Emson PC. Projection subtypes of rat neostriatal matrix cells revealed by intracellular injection of biocytin. J. Neurosci. 1990; 10:3421–3438. [PubMed: 1698947]
9. Surmeier DJ, Mercer JN, Chan CS. Autonomous pacemakers in the basal ganglia: who needs excitatory synapses anyway? Curr. Opin. Neurobiol. 2005; 15:312–318. [PubMed: 15916893]
10. Gatev P, Darbin O, Wichmann T. Oscillations in the basal ganglia under normal conditions and in movement disorders. Mov. Disord. 2006; 21:1566–1577. [PubMed: 16830313]
11. Boyden ES, Zhang F, Bamberg E, Nagel G, Deisseroth K. Millisecond-timescale, genetically targeted optical control of neural activity. Nat. Neurosci. 2005; 8:1263–1268. [PubMed: 16116447]
12. Adamantidis AR, Zhang F, Aravanis AM, Deisseroth K, de Lecea L. Neural substrates of awakening probed with optogenetic control of hypocretin neurons. Nature. 2007; 450:420–424. [PubMed: 17943086]
13. Arenkiel BR, et al. In vivo light-induced activation of neural circuitry in transgenic mice expressing channelrhodopsin-2. Neuron. 2007; 54:205–218. [PubMed: 17442243]
14. Huber D, et al. Sparse optical microstimulation in barrel cortex drives learned behaviour in freely moving mice. Nature. 2008; 451:61–64. [PubMed: 18094685]
15. Sohal VS, Zhang F, Yizhar O, Deisseroth K. Parvalbumin neurons and gamma rhythms enhance cortical circuit performance. Nature. 2009; 459:698–702. [PubMed: 19396159]
16. Cardin JA, et al. Driving fast-spiking cells induces gamma rhythm and controls sensory responses. Nature. 2009; 459:663–667. [PubMed: 19396156]
17. Gong S, et al. Targeting Cre recombinase to specific neuron populations with bacterial artificial chromosome constructs. J. Neurosci. 2007; 27:9817–9823. [PubMed: 17855595]
18. Ouimet CC, Langley-Gullion KC, Greengard P. Quantitative immunocytochemistry of DARPP-32-expressing neurons in the rat caudatoputamen. Brain Res. 1998; 808:8–12. [PubMed: 9795103]
19. Tepper JM, Bolam JP. Functional diversity and specificity of neostriatal interneurons. Curr. Opin. Neurobiol. 2004; 14:685–692. [PubMed: 15582369]
20. Kreitzer AC. Physiology and pharmacology of striatal neurons. Ann. Rev. Neurosci. 2009; 32:127–147. [PubMed: 19400717]
21. Kreitzer AC, Malenka RC. Endocannabinoid-mediated rescue of striatal LTD and motor deficits in Parkinson's disease models. Nature. 2007; 445:643–647. [PubMed: 17287809]
22. Gradinaru V, et al. Targeting and readout strategies for fast optical neural control in vitro and in vivo. J. Neurosci. 2007; 27:14231–14238. [PubMed: 18160630]
23. Gerfen CR, et al. D1 and D2 dopamine receptor-regulated gene expression of striatonigral and striatopallidal neurons. Science. 1990; 250:1429–1432. [PubMed: 2147780]
24. Schwarting RK, Huston JP. Unilateral 6-hydroxydopamine lesions of mesostriatal dopamine neurons and their physiological sequelae. Prog. Neurobiol. 1996; 49:215–266. [PubMed: 8878304]
25. Bergman H, Wichmann T, DeLong MR. Reversal of experimental parkinsonism by lesions of the subthalamic nucleus. Science. 1990; 249:1436–1438. [PubMed: 2402638]

26. Bergman H, Wichmann T, Karmon B, DeLong MR. The primate subthalamic nucleus. II. Neuronal activity in the MPTP model of parkinsonism. J. Neurophysiol. 1994; 72:507–520. [PubMed: 7983515]

27. Mallet N, Ballion B, Le Moine C, Gonon F. Cortical inputs and GABA interneurons imbalance projection neurons in the striatum of parkinsonian rats. J. Neurosci. 2006; 26:3875–3884. [PubMed: 16597742]

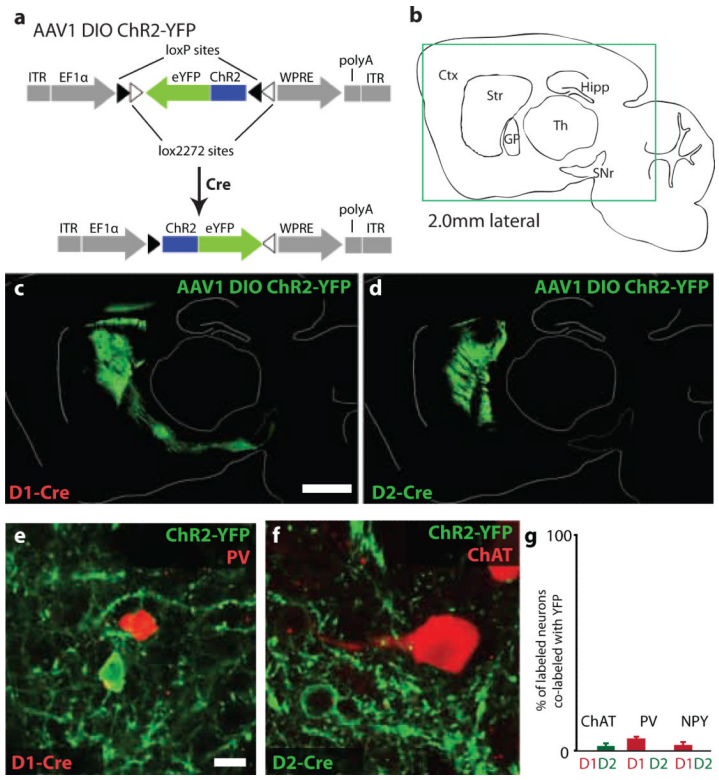

Figure 1. Selective viral-mediated ChR2 expression in striatal direct- or indirect-pathway MSNs

(a) Schematic of the double-floxed Cre-dependent AAV vector expressing ChR2-YFP under control of the EF1α promoter. ITR, inverted terminal repeat; WPRE, woodchuck hepatitis virus post-transcriptional regulatory element. **(b)** Sagittal mouse brain schematic. Ctx, cortex; Str, striatum; GP, globus pallidus; SNr, substantia nigra pars reticulata; Th, thalamus; Hipp, hippocampus. Box indicates region shown in panels c and d. **(c)** Sagittal section showing striatal direct-pathway MSNs expressing ChR2-YFP following injection of Cre-dependent AAV into D1-Cre BAC transgenic mice. Direct-pathway MSN axons target the SNr. **(d)** Expression of ChR2-YFP in striatal indirect-pathway MSNs of D2-Cre BAC transgenic mice. Indirect-pathway MSN axons target the GP. Scale bars in c and d are 1 mm. **(e-f)** Examples of ChR2-YFP-expressing neurons that do not co-express interneuronal markers PV or ChAT. Scale bars in e-f are 15 μm. **(g)** Percent of ChAT, PV, or NPY neurons that co-express ChR2-YFP. Error bars are SEM.

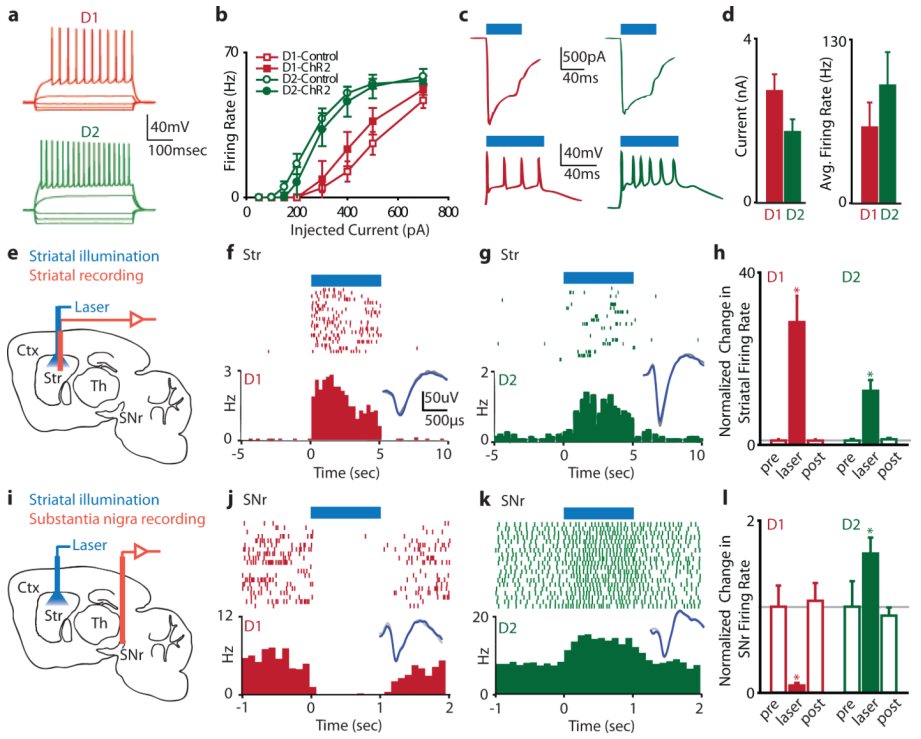

Figure 2. ChR2-mediated excitation of direct- and indirect-pathway MSNs *in vivo* drives activity in basal ganglia circuitry

(a) Whole-cell current-clamp recordings from ChR2-YFP+ neurons *in vitro* demonstrate normal current-firing relationships consistent with D1-MSNs (red traces) or D2-MSNs (green traces) (D1-Control, n=10; D1-ChR2, n=3; D2-Control, n=7; D2-ChR2, n=3). **(b)** Firing rate plotted as a function of injected current in D1-MSNs or D2-MSNs expressing either GFP or ChR2-YFP. **(c)** ChR2-mediated photocurrents (top) and spiking (bottom) in D1 (left) and D2 (right) MSNs. In this and subsequent panels, blue bars indicate illumination time. **(d)** Summary of ChR2-mediated photocurrents (left) and spiking (right) for D1-ChR2 (n=5) and D2-ChR2 (n=4) cells. **(e)** Schematic of *in vivo* optical stimulation and recording in the striatum (Str). Cortex (Ctx), thalamus (Th), substantia nigra pars reticulata (SNr). **(f)** An example MSN recorded from the striatum of an anesthetized D1-ChR2 mouse that displayed increased firing in response to illumination. Insets in f-g and j-k show spike waveform with illumination (blue) or without illumination (grey). Scale bar applies to insets in f-g and j-k. **(g)** An example of a light-sensitive MSN from a D2-ChR2 mouse. **(h)** Normalized change in MSN firing rates in response to striatal illumination in D1-ChR2 (n=16) or D2-ChR2 (n=10) mice. **(i)** Schematic of *in vivo* optical stimulation in striatum and recording in SNr. **(j)** An example of a SNr neuron recorded from a D1-ChR2 mouse that was inhibited by direct pathway activation. **(k)** An example of a SNr neuron recorded from a D2-ChR2 mouse that was excited by indirect pathway activation. **(l)** Normalized change in SNr firing rate in response to activation of the direct (D1, n=8) or indirect (D2, n=4) pathways. Error bars are SEM.

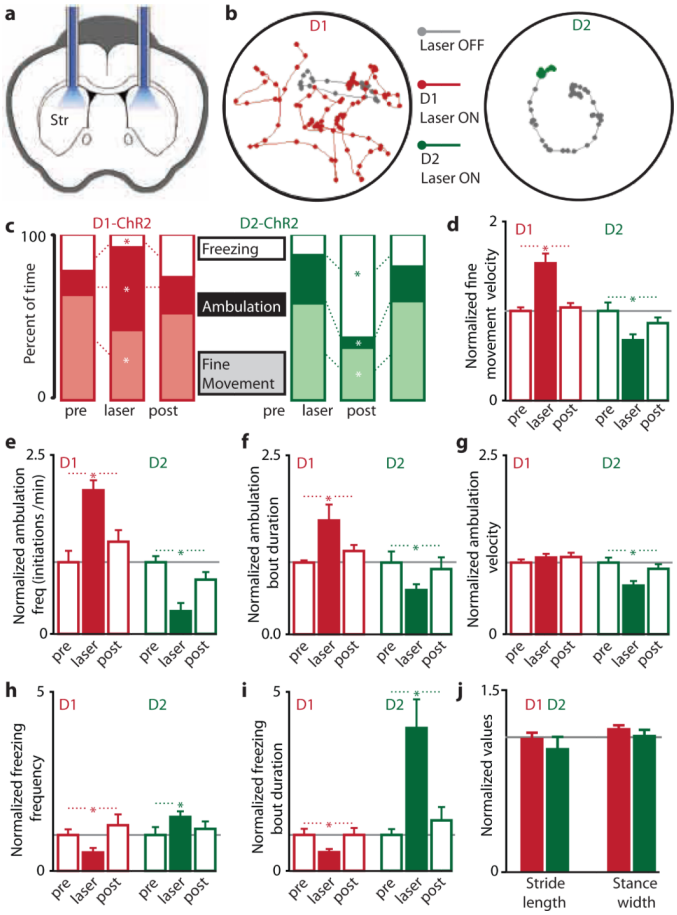

Figure 3. ***In vivo*** **activation of direct or indirect pathways reveals pathway-specific regulation of motor function**

(a) Coronal schematic of cannula placement and bilateral fiber optic stimulation. **(b)** Example of altered motor activity during bilateral striatal illumination in D1-ChR2 (left) or D2-ChR2 (right) mice. Lines represent the mouse's path; dots represent the mouse's location every 300 ms. Grey path represents 20 s of activity prior to illumination; colored paths are 20 s during subsequent illumination. **(c)** Motor activity before (pre), during (laser), and after (post) bilateral striatal illumination in D1-ChR2 (left, red) or D2-ChR2 (right, green) mice. Effect of illumination on **(d)** the velocity of fine movements, **(e)** initiation of ambulatory bouts, **(f)** ambulation bout duration, **(g)** ambulation velocity, **(h)** frequency of freezing, and **(i)** duration of freezing bouts, in D1-ChR2 (red bars, n=9) and D2-ChR2 (green bars, n=8) mice. **(j)** No change in gait in response to illumination in D1-ChR2 (red bars, n=4) or D2-ChR2 (green bars, n=5) mice. Error bars are SEM.

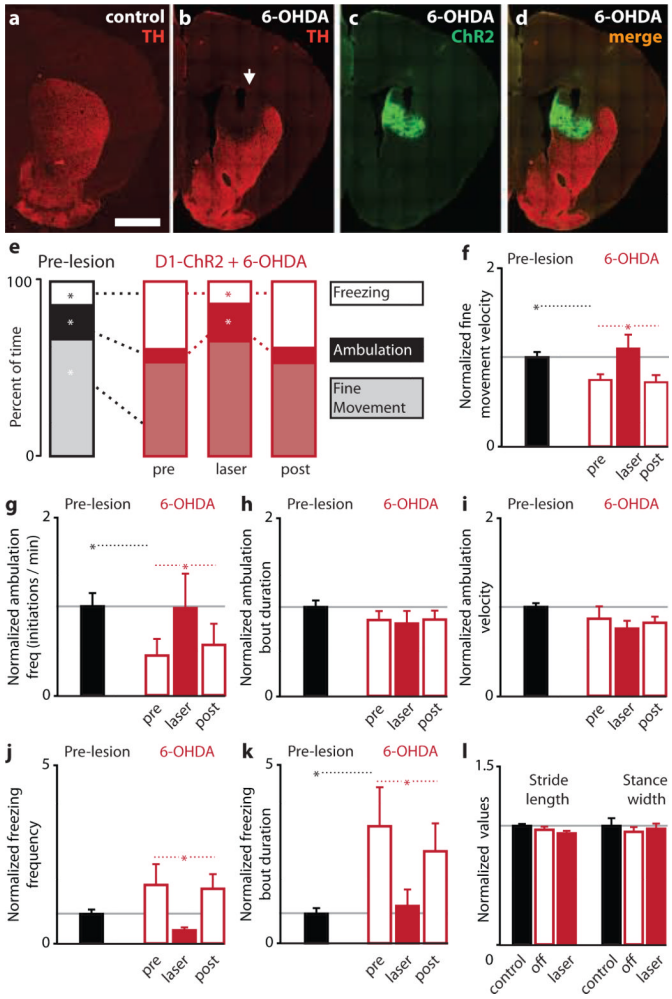

Figure 4. Direct pathway activation rescues motor deficits in the 6-OHDA model of Parkinson's disease

(a) Visualization of striatal dopaminergic afferents by tyrosine hydroxylase (TH) staining in coronal slices. Scale bar is 1 mm. **(b)** Loss of dopaminergic innervation in dorsomedial striatum 1 week after 6-OHDA injection. Arrow marks the injection site. **(c)** ChR2-YFP expression in dorsomedial striatum of 6-OHDA-lesioned mice. **(d)** Merged image shows overlap of ChR2 expression with the 6-OHDA lesion. **(e)** Motor behavior before (left, black bars) and after 6-OHDA lesion (right, red bars) in D1-ChR2 mice (n=10). In 6-OHDA lesioned mice, behavior is shown before (pre), during (laser), and after (post) activation of the direct pathway. Effect of 6-OHDA lesion and direct pathway rescue on **(f)** fine movement velocity, **(g)** initiation of ambulatory bouts, **(h)** ambulation bout duration, **(i)** ambulation velocity, **(j)** frequency of freezing, and **(k)** duration of freezing bouts. **(l)** No change in gait was observed after 6-OHDA lesion or direct pathway activation. Error bars are SEM.